Advances in Nano Research, *Vol. 18, No. 1 (2025) 19-31*
https://doi.org/10.12989/anr.2025.18.1.019

Experimental and analytical investigation of free vibration of a crack FG beam reinforced with alumina nano particles

Raghad Azeez Neamah*[1], Ameen Ahmed Nassar[2], Luay S. Alansari[1], Emad Kadum Njim[3] and Royal Madan[4**]

[1]*Department of Mechanical Engineering, Faculty of Engineering, University of Kufa, Iraq*
[2]*Department of Mechanical Engineering, College of Engineering, University of Basrah, Iraq*
[3]*Ministry of Industry and Minerals, State Company for Rubber and Tires Industries, Najaf, Iraq*
[4]*Department of Mechanical Engineering, Graphic Era (Deemed to be University), Dehradun 248002, Uttarakhand, India*

(*Received September 26, 2024, Revised December 14, 2024, Accepted December 16, 2024*)

Abstract. The crack defect is the main problem that occurs in any structure so the effect of crack dimensions on the free vibration of the functionally graded beam (FGB) is studied theoretically and experimentally. This crack is designed as a notch on the top surface of FGB, which is designed based on Euler and Timoshenko beam theories. In this work, FGB consists of five layers in the thickness direction according to the power law model with different percentages of nano Al_2O_3 and epoxy. Eighteen tensile samples were prepared using a mixture of epoxy Quickmast 105 and nano alumina (Al_2O_3) at volume fractions of 0%, 1%, 2%, 3%, 4%, and 5%. The experiment aimed to determine the nano alumina volume fraction at which the elastic modulus begins to decrease. Then, this beam is prepared from epoxy and alumina Al_2O_3 nano with different percentages by hand lay-up method to measure the natural frequency. The effect of nano percentage, power index value, and crack dimensions is studied extensively. The results revealed that at a 5% volume fraction of nano alumina (Al_2O_3), the elastic modulus increased by 107.12% compared to the pure epoxy sample, while the tensile strength decreased by 16.41% compared to the sample with a 4% volume fraction of nano alumina. Additionally, at a 4% volume fraction, the tensile strength showed an 86.41% increase compared to the pure epoxy sample. Furthermore, when the crack depth ratio and crack position ratio are both 0.5, the natural frequency decreases by 23.30% compared to the intact beam designed with five index values. Finally, the theoretical and experimental results show good agreement, with a maximum difference of 5%.

Keywords: crack; Euler and Timoshenko beam; free vibration; functionally graded beam; mathematical model

1. Introduction

Functionally graded material (FGM) is a special kind of composite material. It consists of two or more dissimilar materials and has a continuous variation of material properties from one phase to another. This variation eliminates the stress concentration found in the laminate composite (Boggarapu *et al*. 2021, Sharma *et al*. 2024, Rallabandi 2024). In engineering design, the choice of material is the important stage. The materials with improved properties are used to meet system requirements, etc. (Bose *et al*. 2023, Chen *et al*. 2022, Lin *et al*. 2021). Few papers studied the influence of cracks on the free vibration of the functionally graded beam (FGB), the cracked beam analysis can be carried out based on different beam theories and in some research, the effect of crack is studied numerically by (Yang and Chen 2008), while presented a theoretical investigation of free vibration behaviour for cracked FGB based on the Euler beam theory and rotational-spring model analytically with different boundary conditions. In (Ke *et al*. 2009), studied the free vibration of FGB containing open edge cracks based on the Timoshenko beam theory analytically. The properties of the materials varied through beam thickness according to the exponential form. Later (Ke *et al*. 2012), studied the nonlinear vibration of cracked FGB dependent on the Timoshenko beam theory. The crack section is modeled by a massless rotational spring. Moreover, in (Sherafatnia *et al*. 2014), investigated the free vibration analysis of cantilever FGB containing open edge crack based on four beam theories, CBT, Rayleigh, and TBT. Two massless rotational and linear springs are used to simulate the crack.

Free vibration analysis was performed by utilizing Iso-Geometric Approach (IGA), a spline-based FEM, and its results were compared with FEM, the Rayleigh-Ritz method, and experimental data for benchmark tests on block and cylinder models. Convergence rate, accuracy, and computational time are compared between IGA and FEM, considering spline order and parameterization effects (Kolman *et al*. 2015). Also, an iso-geometric method offers the advantage of accurately representing mesh geometry through a connection between CAD and NURBS shape functions (Cottrell *et al*. 2006, Hughes *et al*. 2005). In (Yang *et al*. 2015), examined the dynamic behaviour of cracked rectangular FGB based on Euler theory and the continuous stiffness beam model. In (Lien *et al*. 2017),

*Corresponding author, Professor,
E-mail: ragada.deibeal@uokufa.edu.iq
**Co-corresponding author, Professor,
E-mail: royalmadan.me@geu.ac.in

ISSN: 2287-237X (Print), 2287-2388 (Online)

studied the free vibration of multiple cracked FG Timoshenko beams. The massless rotational spring model establishes vibration equations for multiple cracked FGB. In (Shabani and Cunedioglu 2020), analyzed the free vibration of a multi-layered symmetric sandwich Timoshenko FGM beam with two cracks using the finite element method. Static analysis of axially functionally graded microtube with porosity was studied using Von-Karman nonlinear theory (Li *et al*. 2021). A stir casting method is one of the known methods employed to fabricate nanocomposites (Huang *et al*. 2022). Depending upon the manufacturing process selected the porosity distribution will change (Berghouti *et al*. 2019, Ebrahimi and Jafari 2017, Hadji and Avcar 2021, Kuma *et al*. 2021).

The effect of the location of a crack in a partially cracked isotropic and FGM micro-plate with non-uniform thickness was studied analytically (Gupta *et al*. 2018). A scaled boundary polygons technique was utilized to investigate stress intensity factor in FGMs (Chiong *et al*. 2014). The effect of interface on a composite layer for non-homogeneous coating on a homogeneous substrate was studied (Chen and Erdogan 1996). On a cracked FG plate subjected to thermal shock, a 2-D analysis was performed by utilizing ABAQUS wherein user subroutines were used to formulate the problem (Burlayenko *et al*. 2016). Stress intensity on multiple cracks on a FG coated orthotropic strip was solved (Monfared and Ayatollahi 2013). In another research (Tam *et al*. 2019) used the finite element method to study the free vibration of cracked FG graphene nanoplates reinforced composite (GPLRC) beams. A crack in an FG beam has a significant impact on the performance of structures (Kanu *et al*. 2019, Sinha and Kumar 2021). Various theories have been studied by researchers namely: the iso-geometric approach (Do and Lee 2019), Generalized differential quadrature finite element method (Viola *et al*. 2013), extended finite element method (Nasirmanesh and Mohammadi 2017), XIGA-based effective approach (Liu *et al*. 2018), meshless method (Bui *et al*. 2018, Kou and Yang 2019), finite element method (Chang *et al*. 2024, Natarajan *et al*. 2011), analytical methods (Al-Shablle M *et al*. 2022, Al-Shablle *et al*. 2023, Jweeg *et al*. 2023, Njim *et al*. 2024) boundary integral equation method (Zhang *et al*. 2003), phase field theory (Duc and Minh 2021), refined beam theory (Hadji *et al*. 2021, 2022), etc to name a few.

Functionally Graded (FG) beams find applications in structures, thermal systems, energy harvesters, sensors, actuators, and more (Tounsi *et al*. 2023a, Gawah *et al*. 2024, Madenci *et al*. 2023, Zhang *et al*. 2023, Sharma *et al*. 2023). Numerous studies have been conducted to analyze the performance of FG structures under combined loading conditions, such as thermal load (Tounsi *et al*. 2023c), hygro-thermal loads (Tounsi *et al*. 2024), magneto-electro (Mangalasseri *et al*. 2023), thermodynamic behavior (Lafi *et al*. 2024), hygro-thermo-mechanical loads (Mudhaffar 2023) etc. Advancements in manufacturing techniques have enabled the fabrication of FG beams using methods like powder metallurgy, centrifugal casting, and additive manufacturing. Powder metallurgy allows for layer-wise grading with precise control over composition changes (Soni 2024). In contrast, centrifugal casting creates a continuously graded structure due to the mold's rotation, which induces particle or phase mobility in the liquid metal. The reinforcement distribution in centrifugal casting is defined by processing parameters, though it lacks the fixed control seen in powder metallurgy. However, this method is particularly suitable for fabricating axisymmetric structures and offers superior properties compared to powder metallurgy. A key limitation of powder metallurgy is the potential for delamination due to differences in the thermo-mechanical properties of the mixed materials. Additive manufacturing has gained prominence as a solution, enabling the production of multiple graded layers with improved bonding to prevent delamination (Bhardwaj and Mishra 2024, Garima *et al*. 2024). During fabrication, porosity can arise due to suboptimal processing conditions. In powder metallurgy, factors such as compaction load, sintering temperature, and sintering time significantly affect product density. Similarly, in casting processes, parameters like mold rotation speed, pouring temperature, and binder selection play critical roles in minimizing porosity (Singh *et al*. 2018, Kumar *et al*. 2020). The effect of porosity in FG plate, beam and sandwich structures was studied for bending, buckling, and free vibration (Alsubaie *et al*. 2024, Boutaleb *et al*. 2024, Alsubaie *et al*. 2023, Al-Houri *et al*. 2024, Belabed *et al*. 2024). Various gradation laws, such as power law (Tounsi *et al*. 2023b), sigmoid law (HHS AlSaid-Alwan *et al*. 2020, Hadji and Avcar 2021) exponential law, and trigonometric law, have been considered for analysis. The choice of gradation law has been found to significantly influence the performance of FG structures (Tahir *et al*. 2022, Kouider *et al*. 2021).

In this work, the free vibration of a new model of FG beam based on Euler and Timoshenko's theories is studied. It is prepared manually using the lay-up method of epoxy and Al_2O_3 nano alumina. The beam consists of five layers in the thickness direction, and the material properties vary in the thickness direction according to the power law model. The effect of power index value and crack dimensions on the free vibration of the beam is studied numerically, analytically, and experimentally. From the host of the literature review, it has been found that no study to date in which fabrication, analytical investigation, and experimentation have been performed. This study benefits structural engineers, materials scientists, vibration analysis researchers, and professionals in aerospace and mechanical engineering by providing new insights into the free vibration behavior of functionally graded beams with varying nano-alumina content.

The work is organized as follows: In Section 2, an analytical model is proposed for FG composite beams with the presence of cracks. In section 3, finite element tools are used to simulate analytical results. However, section four presents experimental work including sample fabrication and conducting mechanical and free vibration tests. The results of the analysis of FG-cracked nanobeam structures are presented in Section 5. Finally, conclusions are given in Section 6.

2. Analytical model

2.1 Problem description and crack modeling

Free vibration is the main problem that occurs with any type of beam. The functionally graded (FG) beam is

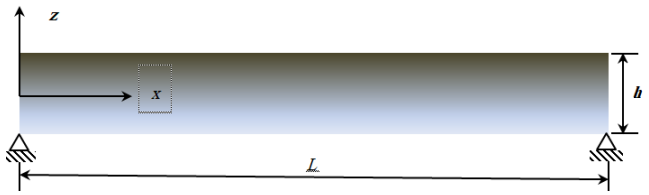

Fig. 1 Geometry of FG beam

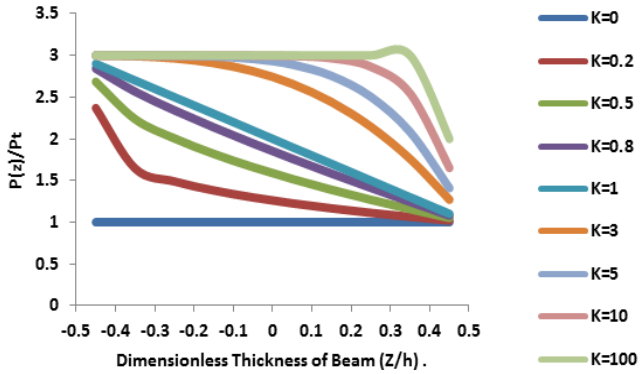

Fig. 2 Variation of material property (p(z)) along thickness of FGB for different values of power–law index (k) when $(\frac{p_b}{p_t} = 3)$

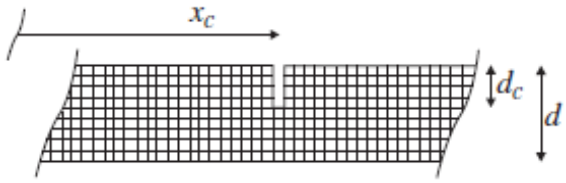

Fig. 3 The simple crack model

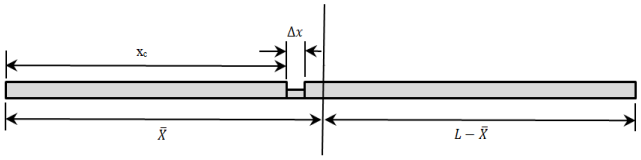

(a) Simply Supported FG Beam with crack

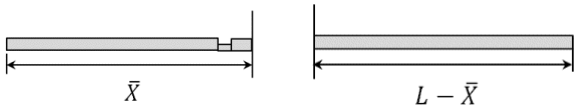

(b) Left Cantilever FGB (c) Right Cantilever FGB

Fig. 4 Dividing Simply supported FGB with crack

suitable to avoid these problems, but the gradation of properties will prevent us from applying classical beam theories, so it needs to advance in the mechanism of application of these theories. Let the dimensions of FGB be length L along the X-direction and square cross-section b*h along the Y and Z-directions respectively as shown in Fig. 1.

This beam is made from two different materials with gradient properties along the thickness direction (i.e. the Z-direction). This gradient in material properties is described according to the power-law model as illustrated in the following equations (Şimşek and Yurtcu 2013).

$$P(z) = (P_t - P_b)(\frac{z}{h} + \frac{1}{2})^K + P_b \quad (1)$$

$$E(z) = (E_t - E_b)(\frac{z}{h} + \frac{1}{2})^K + E_b \quad (2)$$

$$\rho(z) = (\rho_t - \rho_b)(\frac{z}{h} + \frac{1}{2})^K + \rho_b \quad (3)$$

where P(z) is the property at any point in thickness of FGB, E(z) and ρ (z) are the elastic modulus and density at any point in thickness of FGB, P_t and P_b are the property of top and bottom materials respectively, (h) is the thickness of FGB and, (k) is the non-negative power index value. The rule of a mixture is used in Eq. (1) to compute the material properties of composite materials:

$$P_t V_t + P_b V_b = P(z) \quad (4)$$

where V_b is the volume fraction of the bottom material and V_t is the volume fraction of the top material

$$V_t = (\frac{z}{h} + \frac{1}{2})^K \quad (5a)$$

in the case of no voids.

$$V_t + V_b = 1 \quad (5b)$$

According to Equation (1), the property at any point in thickness of FGB (P(z)) such as Elastic modulus (E), density (ρ), Poisson ratio (ν), and shear modulus (G) depending on the properties of top and bottom materials (P_t and P_b). The variation of properties along the thickness direction based on the power index is shown in Fig. 2.

In a homogeneous beam, the crack effect is considered by calculating the stiffness EI (Friswell and Penny 2002):

$$EI(x) = \frac{(EI)_0}{1 + C\exp(\frac{-2\alpha|x - x_c|}{d})} \quad (6a)$$

The second moment of area for intact and cracked beam consists of parameter C and the constant $\alpha = 0.667$ is defined as:

$$Io = \frac{wd^3}{12}, Ic = \frac{w(d-dc)^3}{12}, C = \frac{(I - Ic)}{Ic} \quad (6b)$$

The depth and width of the intact beam are defined as (d and w), while the crack depth is defined as (d_c), see Figure 3. The position along the beam is defined as x, while the crack position is defined as x_c as:

The cracked FG beam is modeled in a different form in the present work. It is made on the beam surface to study its effect on the natural frequency of the FG beam. The presence of a crack represents a change in beam stiffness and geometry, essentially the beam thickness. This beam is divided into three regions to represent the crack effect as a change in thickness for FGB. The first is the crack region, as shown in Fig. 3. In this region, the second moment of area and the modulus of elasticity are varied according to Eq. (6). The second and third regions are the left and right regions of the crack, and their properties are approximately constant along the axial direction. Still, their properties vary along the thickness of the FGB. The first step is to calculate the equivalent second moment of area (I) of a supported beam, the centroid ($\bar{X}$) of the beam, and it is calculated as:

Let V be the volume of the region where Δx is the crack width. Due to the crack position and crack dimensions,

the centroid ($\bar{X}$) of the FGB is changed. According to the new centroid position ($\bar{X}$), the FGB is divided into two cantilever beams, as shown in Fig. 4.

After calculating the centroid for the system, the supported beam becomes a two-cantilever beam with different lengths. So, two lengths (left, right) and two equivalent second moments of area (I_{eq_l}, I_{eq_R}). Finally, the equivalent second moment of area for a simply supported beam is:

$$(I)_{eq} = \frac{(L_R + L_l) * (L_R)^2 * (L_l)^2}{\left(\left(\sum_{n=1}^{N\,right} \frac{{l_{n-1}}^3 - {l_n}^3}{(I)_n}\right) * {L_R}^2\right) + \left(\left(\sum_{n=1}^{N left} \frac{{l_n}^3 - {l_{n-1}}^3}{(I)_n}\right) * {L_l}^2\right)} \quad (7)$$

where, $L_R = L - \bar{X}$ and it is the length of the right beam and $L_l = \bar{X}$ is the length of the left beam. According to Equation (7), for each crack position and crack depth, the equivalent beam thickness is calculated as below:

$$h_{eq} = \sqrt[3]{12 * \frac{I_{eq}}{width}} \quad (8)$$

This thickness is used in all the above models to analyze the cracked FG beam using three theories (CBT, TBT, and HOSDT). In this study, the beam's deformation is assumed in the x-z plane. The axial, vertical, and transverse displacements of any point of the beam are denoted by U, V, and W, respectively. According to the shear deformation theory, the displacement field is taken as (Neamah *et al*. 2022).

The functions in question rely heavily on the invariants of the deformation tensor, effectively quantifying the extent of material stretching or compression across diverse directions.

$$\begin{aligned} u(x,z,t) &= u(x,t) - z\frac{dw}{dx} + f(z).u1(x,t) \\ v(x,z,t) &= 0 \\ w(x,z,t) &= w(x,t) \end{aligned} \quad (9)$$

where (u and w) are the axial and transverse displacements of any point on the neutral axis, while (u_1) is a function that represents the effect of transverse shear strain on the middle surface of the beam. The shape function f(z) determines the distribution of the transverse shear strain and stress through beam thickness. Classical beam theory (CBT) is applied when the shape function equals zero. The present study also uses two shape functions: Timoshenko beam theory (TBT) and high-order shear deformation theory (HOSDT). The shape functions in each theory are presented and for free vibration, all equations of motion are created by Hamilton's principle.

$$\int_{t1}^{t2} (\delta K - \delta U_{int} - \delta W_{ext})\, dt = 0 \quad (10)$$

where δU_{int} , δW_{ext} and δK are the variations of strain energy, external work, and kinetic energy as represented in (Hadji *et al*. 2024, Madan *et al*. 2024, Raad *et al*. 2024, Singh *et al*. 2024). The solution of governing equations of free vibration according to Timoshenko beam theory (TBT) and (HOSDT) is as,

$$\left(-\begin{bmatrix} -\alpha^2 A_{11} & \alpha^3 B_{11} & -\alpha^2 E_{11} \\ \alpha^3 B_{11} & -\alpha^4 D_{11} & -\alpha^3 F_{11} \\ -\alpha^2 E_{11} & \alpha^3 F_{11} & -\alpha^2 H_{11} - A_{55} \end{bmatrix} - {\omega^2}_n \begin{bmatrix} m_{00} & -\alpha m_{11} & m_f \\ -\alpha m_{11} & -\alpha^2 m_{22} + m_{00} & -\alpha m_{fz} \\ m_{00} & -\alpha m_{fz} & {m^2}_f \end{bmatrix}\right)\begin{bmatrix} U_n \\ W_n \\ G_n \end{bmatrix} = \begin{bmatrix} 0 \\ 0 \\ 0 \end{bmatrix} \quad (11)$$

While the solution of governing equations of free vibration according to (CBT) can be written as (Neamah *et al*. 2024),

$$\left(-\begin{bmatrix} (-\alpha^2 A_{11}) & (\alpha^3 B_{11}) \\ (\alpha^3 B_{11}) & (-\alpha^4 D_{11}) \end{bmatrix} - {\omega_n}^2 \begin{bmatrix} m_{00} & -m_{11}\alpha \\ -m_{11}\alpha & m_{22}\alpha^2 \end{bmatrix}\right)\begin{bmatrix} U_n \\ W_n \end{bmatrix} = \begin{bmatrix} 0 \\ 0 \end{bmatrix} \quad (12)$$

These equations can be solved by FORTRAN program to get the value of natural frequency.

3. Numerical model

A three-dimensional model (3D) for an intact and cracked FG beam is drawn in ANSYS APDL software. The dimensions of this beam are length, width, and thickness in X, Z, and Y directions, respectively. This beam is drawn with five layers in a thickness direction. Each layer has a thickness equal to the thickness of the beam over the number of layers. The material properties of each layer are calculated according to the experimental tensile test data. The elastic modulus and density of the top and bottom surfaces of the FG beam are calculated, according to these values, the elastic modulus and thickness of each layer are calculated using the power law model**.** The effect of power index value (k=0.5, 1, and 5), crack position ratio (L_c/L=0.1, 0.2, 0.3, 0.4 and 0.5), and crack depth ratio (h_c/h= 0.1, 0.2, 0.3, 0.4 and 0.5) on the free vibration is studied. In this simulation, it was assumed that the crack leads to a decrease in the elastic modulus of each layer in the crack region, and this decrease is calculated by using Equation 6. The equivalent moment of inertia is automatically decreased and calculated using ANSYS software.

3.1 Numerical simulation of cracked FG beam

For free vibration analysis, the FG beam is designed with five layers in a thickness direction and three regions: left crack, proper crack, and crack region. These layers are merged using (glue) from preprocessing in ANSYS software. The material properties of layers on the left and right sides of the crack region have the same properties of intact FG beam. In contrast, the modulus of each layer in the crack region is decreased according to the crack depth ratio and crack position ratio, which are calculated from Eq. (6). In this simulation, the crack is represented by cutting off the upper part of the FG beam with (1 mm) width and different depth and position according to the studied cases so that the reduction of the moment of inertia is automatically developed by ANSYS software. Fig. 5 illustrates the shape of the cracked beam when the power index is 0.5 and the crack position ratio and crack depth ratio are 0.1. For free vibration analysis, the FG beam is designed with five layers in a thickness direction and three

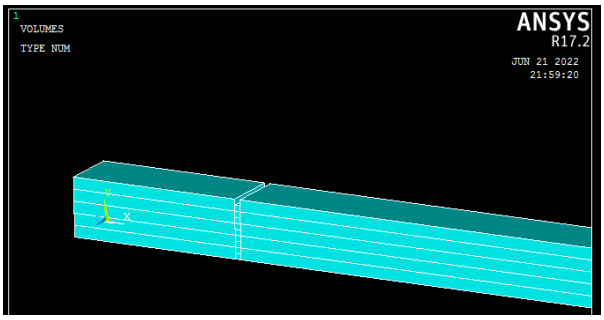

Fig. 5 Cracked FG beam when the crack position ratio and crack depth ratio = 0.1

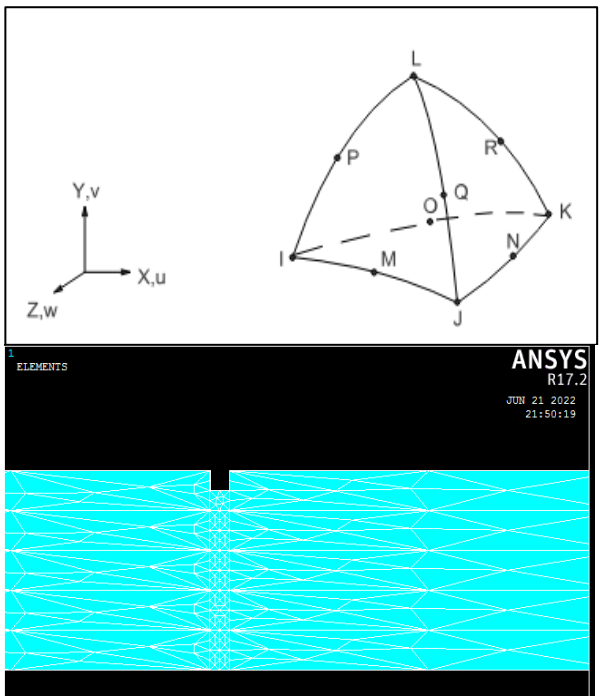

Fig. 6 Element geometry and meshing of five layers for a three-dimensional model

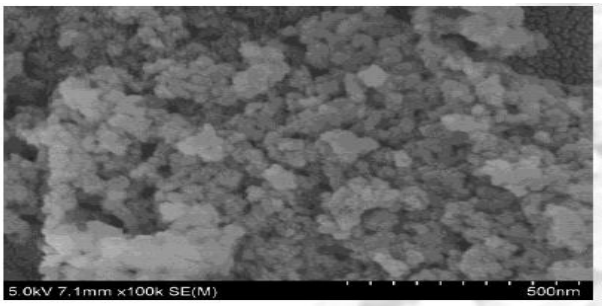

Fig. 7 SEM for nano Al_2O_3

Table 1 Nano (α phase) Al_2O_3

Property	Concentration	Particle size (nm)	Density (g/cm^3)
Value	99.9%	50-90	3.95

Table 2 Quick mast 105 epoxy properties from the supplier

Compressive strength (MPa)	Flexural strength (MPa)	Tensile strength (MPa)	Density (g/cm^3)	Poisson ratio
50	82	28	1.15	0.33

regions: left crack, proper crack, and crack region. These layers are merged using (glue) from preprocessing in ANSYS software. The material properties of layers on the left and right sides of the crack region have the same properties of intact FG beam.

In contrast, the modulus of each layer in the crack region is decreased according to the crack depth ratio and crack position ratio, which are calculated from Eq. (6). In this simulation, the crack is represented by cutting off the upper part of the FG beam with (1mm) width and different depth and position according to the studied cases so that the reduction of the moment of inertia is automatically developed by ANSYS software. Fig. 5 illustrates the shape of the cracked beam when the power index is 0.5 and the crack position ratio and crack depth ratio are 0.1.

After completing the building of the intact and cracked (3D) FGB model, the material properties of each layer were entered into the ANSYS program. A solid Tetrahedral 10 node 187 element was used for meshing, and each layer of this beam was meshed according to its material properties and dimensions, as shown in Fig. 6.

4. Experimental work

This study presents the experimental work in detail. It illustrates the steps of preparing an FG beam and includes the measuring process for the natural frequency of intact and cracked FG beams.

The steps of experimental work are divided into the following:

• Prepare an acrylic tensile mold to produce eighteen samples. Each sample consists of a mixture of epoxy Quickmast 105 base type and nano-alumina Al_2O_3 with different volume fractions (0, 1, 2, 3, 4, and 5) %.

• Measure each sample's elastic modulus and tensile strength to find the saturation percentage of alumina from which the tensile strength starts to decrease and the highest value of elastic modulus (i.e., the critical volume fraction of nano-alumina Al_2O_3).

• Design and prepare an acrylic open mold to produce a new model of FG beam. This beam is prepared from five layers in the thickness direction. Each layer has a 2 mm thickness and consists of a mixture of different percentages of epoxy resin and alumina Al_2O_3 by hand lay-up method. These percentages of epoxy and nano are dependent on tensile results and power index value.

4.1 Materials used in current work

The materials used in this work are:

• Nano Al_2O_3 from (Rabie Sky Spring Company) is used as reinforced material, and its technical properties and SEM are illustrated in Table (1) and Fig. (7), respectively.

• Quickmast 105 base epoxy resin is used as a matrix and becomes solid by adding the hardener in a 4:1.47 ratio. Table 2 illustrates the technical properties of this epoxy.

4.2 Tensile test

An acrylic tensile mold is prepared by a CNC laser machine according to ASTM D638, as shown in Fig. 8,

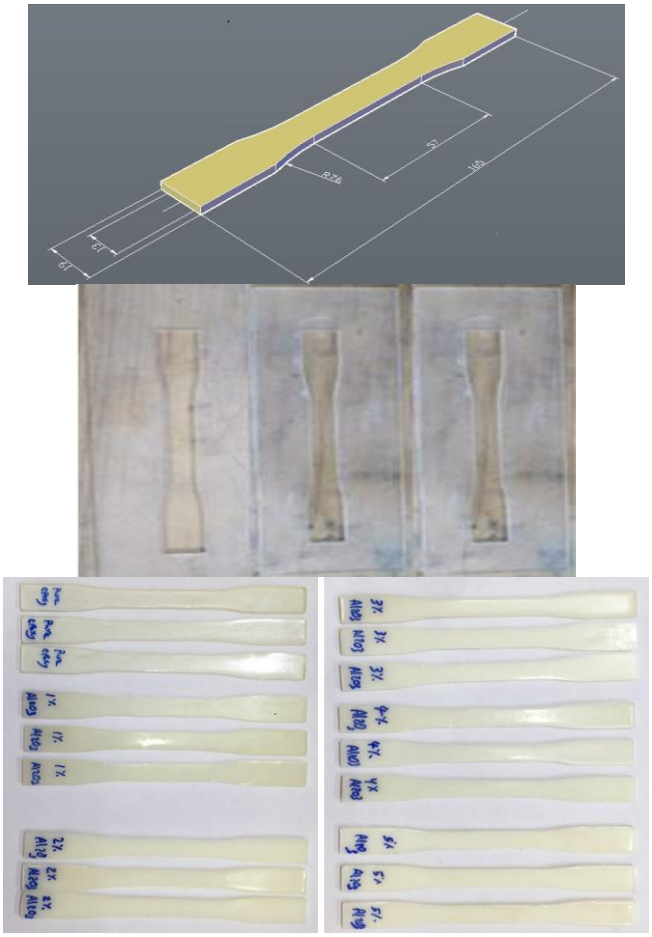

Fig. 8 Tensile specimen (ASTM D638) and acrylic tensile mold

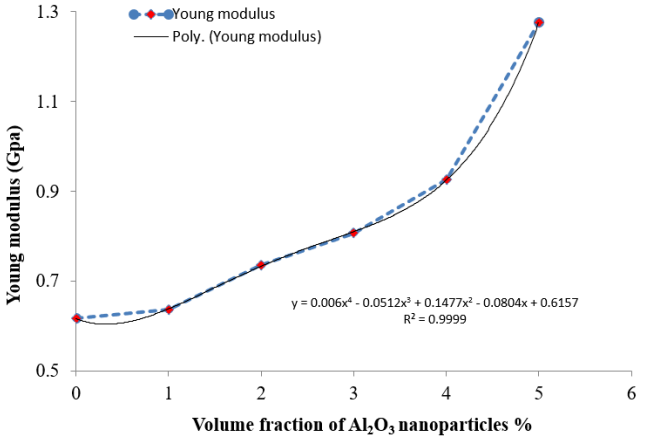

(a) Elastic modulus versus volume fraction percentage

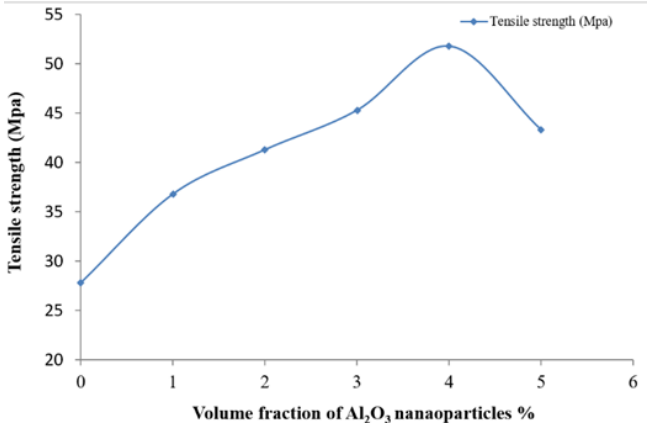

(b) Tensile strength versus volume fraction percentage

Fig. 9 The elastic modulus and Tensile strength versus volume fraction percentage

with a 3 mm thickness. Eighteen homogenous tensile samples are produced by mixing epoxy with (0, 1, 2, 3, 4, and 5) % of Al_2O_3 (three samples for each percent) depending on volume fraction (V_f) percentage. The first three samples are produced from pure epoxy mixed manually with a hardener for five minutes. The other samples are made from Al_2O_3 with different percentages and mixed with epoxy using an electric mixer for several minutes till homogeneity is achieved. This mixture is entered into an ultrasonic mixture device to disperse the nanomaterial. The volume of Al_2O_3 (V_{nano}) and the volume of polymer ($V_{polymer}$) (volume of epoxy and volume of hardener) is calculated by multiplying its volume fraction (V_f) by the volume of mold (V_{mold}). The mass of Al_2O_3 (m_{nano}) in each sample is calculated by multiplying its density (ρ_{nano}) by the volume of nano (V_{nano}). After mixing, the hardener is added, and the mixture is mixed for five minutes. The mixture is then poured into the tensile molds. The preparation steps of the tensile samples occurred at room temperature. The tensile samples are removed from the mold after one day, and the uniaxial tension tests are carried out on these specimens with head speed (2 mm/min) to calculate their elastic modulus and tensile strength, as shown in Fig. 9. A universal test device uses a 5KN maximum load capacity at Babylon University.

4.3 Manufacturing FG beam by hand lay-up method

A nine acrylic open mold is fabricated by a CNC machine with dimensions of (300mm*10mm*10mm) as shown in Fig. 10. Some calculations in this study are dimensionless, and any dimensions may be taken. The hand lay-up method produces a stepwise epoxy-alumina FG beam with five layers in a thickness direction. Each layer has a 2 mm thickness and a different percentage of epoxy and Al_2O_3. Its simplicity and low tooling cost characterize the hand lay-up method. Sixteen screws and silicone material are used to connect the two pieces of the mold well to prevent leakage of the mixture. Usually, to get the product quickly, the mold is coated with wax by a piece of cotton. Three kinds of FG beams based on the value of power law are prepared with five layers from different percentages of epoxy and alumina. The epoxy is mixed with Al_2O_3 in all layers according to the percentages calculated according to tensile test results given by Eq. (2). This mixture is mixed for several minutes by a mechanical mixer and then entered into an ultrasonic mixture device for 30 minutes to disperse the alumina and remove the bubbles. The hardener is added to the mixture and well mixed for five minutes. Mixing steps for the layers and all values of the power index have the same procedure but with different

Fig. 10 The model of FG beam

Fig. 11 FGB samples

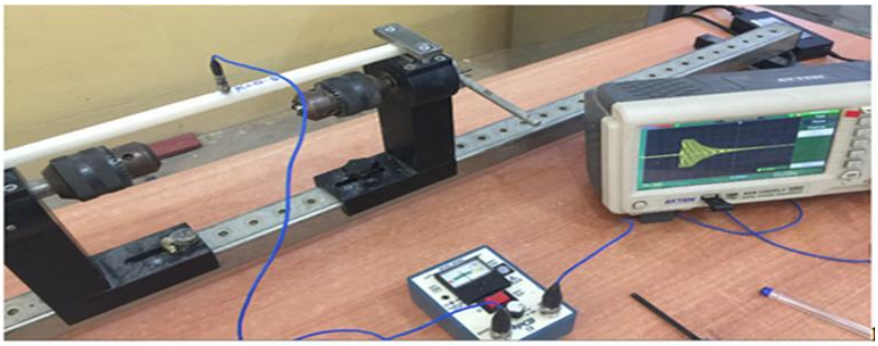

Fig. 12 FG beam under free vibration test

Table 3 Preparing the first model of the FG beam when the power index is 0.5

Layer	V_f % of Al_2O_3	Time of mechanical mixing	Time for pouring next layer	Final Level
First	(2.3%)	(20 minutes)	until becomes a gel	(2mm)
Second	(4.2%)	(30 minutes)	until becomes a gel	(4mm)
Third	(4.6%)	(35 minutes)	until becomes a gel	(6mm)
Fourth	(4.8%)	(40 minutes)	until becomes a gel	(8mm)
Fifth	(4.9%)	(45 minutes)	until becomes a gel	(10mm)

percentages of epoxy and Al_2O_3. The value of elastic modulus for each layer is also measured in a tensile test to improve the validity of the present model. For example, when the index value is 0.5, the mixing steps are presented in Table 3. After mixing and pouring all layers, the product is left for a whole day, and then it is extracted from the mold manually, as shown in Fig. 11. The natural frequency is measured experimentally for intact and cracked FG beams in a mechanical laboratory at the University of Kufa.

4.4 Free vibration test

The vibration test rig is composed of the following parts: hammer, accelerometer, amplifier, and digital storage oscilloscope. The output data from the digital storage oscilloscope are saved to a removable disc and then simulated by using a sig-view program to calculate the value of natural frequency. The effect of crack depth ratio when (L_c/L) is 0.5 for all index values are tested, and the FGB during testing is illustrated in Fig. 12.

Table 4 Comparison of frequency ratio (ω_c/ω_{int})

Lc/L	Theories						
	Present (ANSYS)	Present (CBT)	Present (TBT)	Present (HSDBT)	Ref. (Lien *et al*. 2017)	Ref. (Khiem *et al*. 2023)	Ref. (Yu and Chu 2009)
0	1	1	1	1	1	1	1
0.1	0.99267	0.99638	0.99640	0.99640	0.997	0.997	0.997
0.2	0.98650	0.98809	0.98815	0.98813	0.99	0.99	0.99
0.3	0.98062	0.97494	0.97507	0.97505	0.982	0.982	0.982
0.4	0.97427	0.95824	0.95845	0.95841	0.975	0.975	0.976
0.5	0.97039	0.94603	0.94630	0.94625	0.972	0.972	0.973

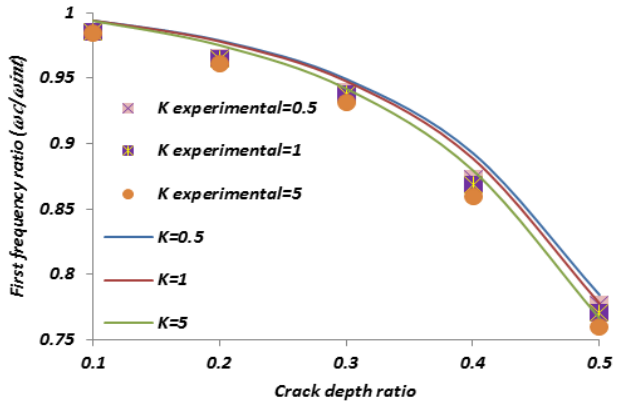

Fig. 13 Validation of frequency ratio with Experimental work

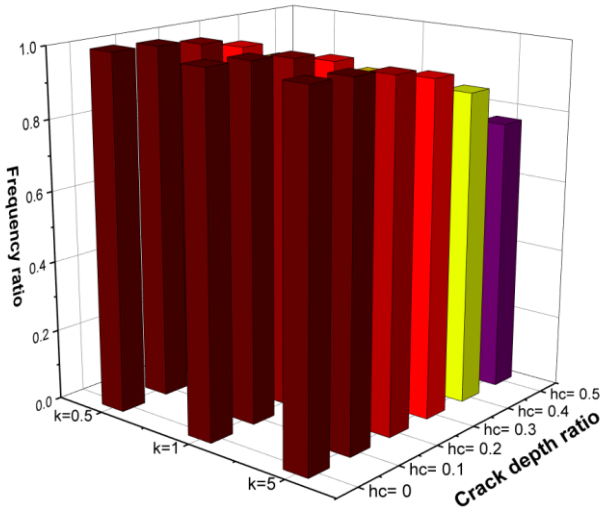

Fig. 14 The effect of the power index value K on the frequency when the crack position ratio Lc/L is 0.5

5. Results and discussion

In this work, a new model of a cracked FG beam is derived based on different beam theories to calculate the free vibration. The effect of different parameters on natural frequency is investigated numerically and analytically. To prove the accuracy of the presented model in predicting the frequency of simply supported FG beam, this model is built with length 1 m, width 0.1 m, thickness 0.05 m, E_b=14 GPa, $v_b = 0.33, \rho_b = 7800$ kg/m^3, E_t=70 GPa, $v_t = 0.33$, $\rho_t = 2780$ kg/m^3 with power index and crack depth ratio (h_c/h) are 2 and 0.2 respectively for different crack position ratios (L_c/L) as recorded in Ref. (Khiem *et al*. 2020, Lien *et al*. 2017, Yu and Chu, 2009). Table 4 presents the frequency ratios (ω_c/ω_{int}) of cracked to intact beam for the present model (Khiem *et al*. 2020, Lien *et al*. 2017, Yu and Chu, 2009). The results agree with the reference found in the literature with few discrepancy percentages.

The natural frequency of manufactured simply supported FGB with a different index value, and other crack depth ratios are calculated experimentally when the crack position ratio (L_c/L) is 0.5. These data are compared with specific numerical findings for the same beam to determine their percentage difference. Fig. 13 illustrates the effect of crack depth ratio (h_c/h) with different index values on the first frequency ratios (ω/ω_{int}) (frequency of cracked to intact supported FGB). From this Figure, it may be concluded that the experimental and numerical results are compatible, and the maximum percentage of the difference between them is 2.2%.

After testing the developed analytical and numerical methods, extensive analytical and numerical work represented by first frequency and first frequency ratio (ω/ω_{int}) are developed. The comparison of the numerical ANSYS results with the analytical results represented by CBT, TBT, and HOSDT was carried out to investigate the effect of crack depth ratio (h_c/h), crack position ratio (L_c/L), and power index value on the behavior of FGB. The impact of five values for the crack depth ratio and crack position ratio (0.1, 0.2, 0.3, 0.4, and 0.5) and three power index values (0.5, 1, and 5) are presented in detail.

Fig. 14 numerically illustrates the power index value's effect on the FG beam's frequency containing a crack in the midpoint at different depths. From this Figure, it can be seen that the frequency becomes lower as the power index value increases from 0.5 to 5. This is because any increase in the power index causes the stiffness of the FG beam to drop. So, the natural frequency of the FG beam with a high index value is more sensitive to the crack presence in FG beams. Fig. 15 shows the effect of the crack depth ratio (h_c/h) on the FG beam's frequency for index k=5, having a single crack at various position ratios. As (h_c/h) increases, it can be observed that the frequency decreases. This is because the stiffness of FGB lowers as the crack depth ratio increases and this reduction shows that the crack depth ratio increases the sensitivity of natural frequency to the crack.

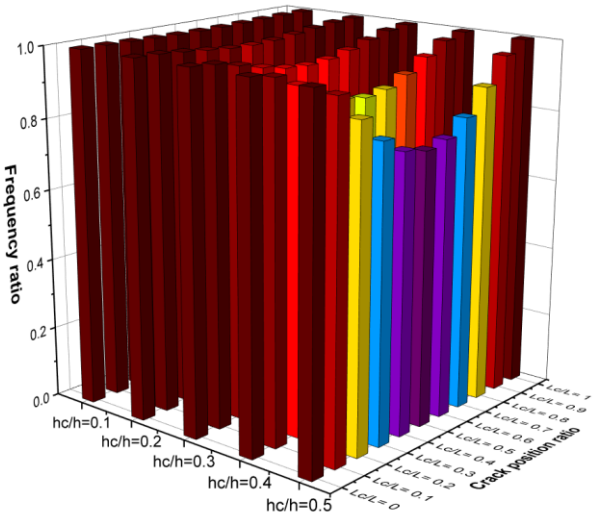

Fig. 15 The effect of the crack depth ratio hc/h on first frequency and first frequency ratio when the power index value K is 5

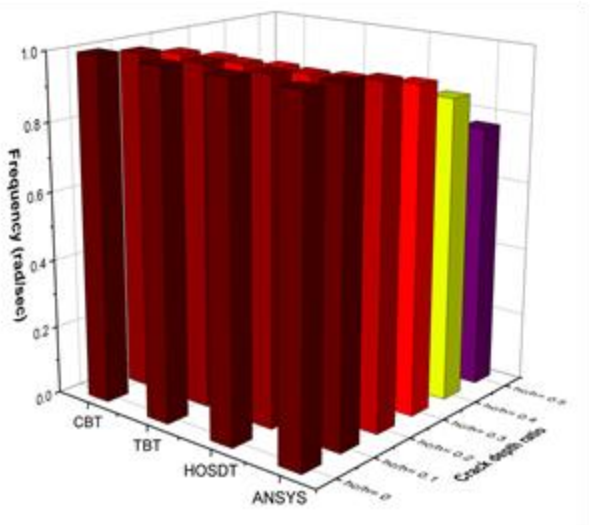

(a)

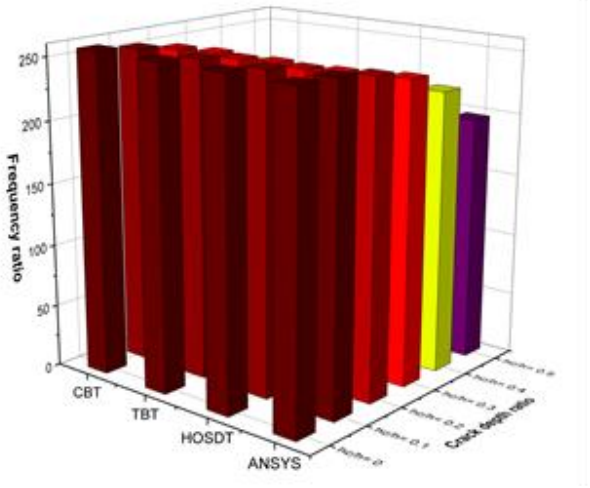

(b)

Fig. 16 (a-b) The effect of deformed theory on first frequency and first frequency ratio when Lc/L is 0.5 and power index value K is 5

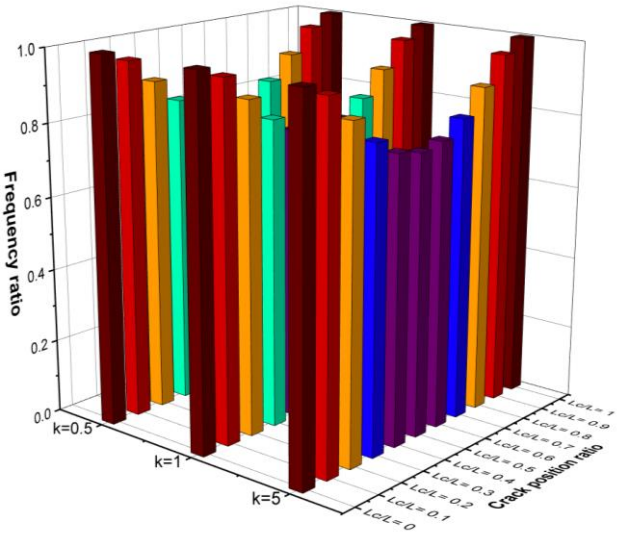

Fig. 17 The effect of the power index value K on first frequency and first frequency ratio when the crack depth ratio (h_c/h) is 0.5 numerically

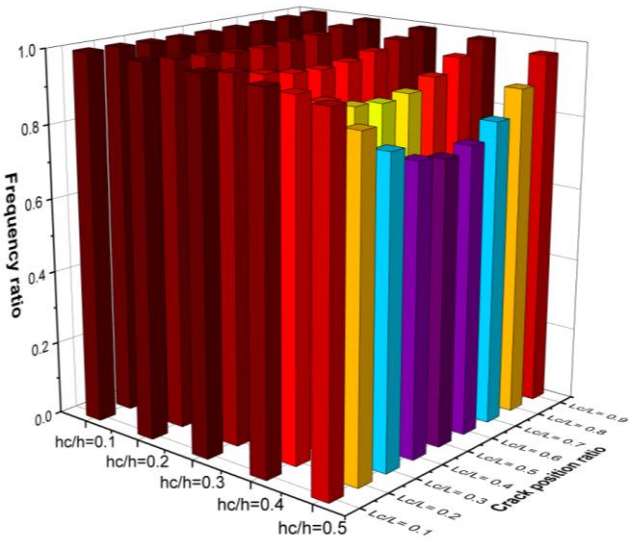

Fig. 18 The effect of crack depth ratio on first frequency and first frequency ratio when the power index value K is 5

Fig. 16 shows the effect of deformed theory on the frequency ratio of FGB with crack for different crack depth ratios and when the power index value and crack position ratio are 5 and 0.5, respectively. It can be seen that the frequency in CBT is greater than that of TBT, HSDBT, and ANSYS. It means that the shear effect leads to a decrease in the frequency of FGB for different crack depth ratios. Fig. 17 presented numerically the impact of power index value on the first frequency and first frequency ratio (ω/ω_{int}) of FGB with a single crack at different positions and when the value of crack depth ratio is 0.5. Fig. 18 illustrates the influence of crack position ratios on the first and first frequency ratios of supported FGB containing a single crack at different crack depth ratios numerically when the power index value is 5. Fig. 19 shows the effect of deformed theory on the frequency and frequency ratio of FGB with

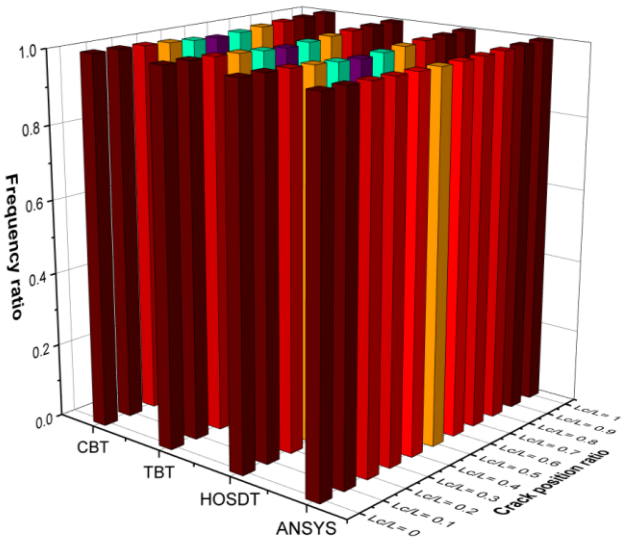

Fig. 19 The effect of deformed theory on first frequency and first frequency ratio when K is 5 and hc/h is 0.5. In general, the trend observed illustrates how key parameters such as material properties, and crack depth affect the frequency of the beam. Increasing the material index reduces the dimensionless frequency. This is because a higher material index, which corresponds to greater stiffness, generally owers the vibration frequency of the plate by increasing its resistance to deformation

crack for different crack position ratios and when the value of power index and crack depth ratio is 5 and 0.5, respectively.

From all the above results, it can be seen that all results are symmetric about the mid-span due to the symmetry of this beam. The crack position ratio significantly affects the frequency FGB with different beam theories, especially when the crack position ratio approaches the midpoint. Moreover, when the crack position ratio is close to the pinned end, the cracked beam's frequency approaches the intact frequency. This is because the midpoint of a supported FGB is the furthest from the pinned end. Finally, the first frequency ratios in CBT are more significant for different crack position ratios than that of TBT, HSDBT, and ANSYS models.

6. Conclusions

In this study, a new FGB model based on different theories (CBT, TBT, and HOSDT) is derived and simulated analytically and numerically. The effect of several parameters on natural frequency is studied. Also, a new model of cracked FGB is designed and prepared with five layers in the thickness direction using the hand lay-up method. Each layer consisted of a different volume fraction percentage of nano Al_2O_3. The effect of crack dimensions and positions is studied analytically, numerically, and experimentally. Based on the results of the intact and cracked FGB and their discussions, the conclusions are as follows:

1. The shear effect in FGB leads to a decrease in the natural frequency.

2. As the crack depth ratio (h_c/h) and crack position ratio (L_c/L) increase, the natural frequency decreases, especially at the midpoint of FGB. When the crack depth ratio and crack position ratio are 0.5, the frequency decreases by 23.3 % from the intact beam when the index value is 5.

3. The increase in power index K from (0.5 to 5) reduces the beam's equivalent stiffness and lowers its natural frequency.

References

Al-Houri, S., Al-Osta, M.A., Bourada, F., Gawah, Q., Tounsi, A. and Al-Dulaijan, S.U. (2024), "Analysis of porosity-dependent wave propagation in FG-CNTRC beams utilizing an integral higher-order shear deformation theory", *Int. J. Struct. Stabil. Dyn.*, 2550233. https://doi.org/10.1142/S0219455425502335

Al-Shablle M., Al-Waily M. and Njim, E.K. (2022), "Analytical evaluation of the influence of adding rubber layers on free vibration of sandwich structure with the presence of nano-reinforced composite skins", *Arch. Mater. Sci. Eng.*, **116**(2), 57-70. https://doi.org/10.5604/01.3001.0016.1190.

Al-Shablle, M., Njim, E.K., Jweeg, M.J. and Al-Waily, M. (2023), "Free vibration analysis of composite face sandwich plate strengthens by Al2O3 and SiO2 nanoparticles materials" *In Diagnostyka*, **24**(2), 1-9. https://doi.org/10.29354/diag/162580

AlSaid-Alwan, H.H.S. and Avcar, M. (2020), "Analytical solution of free vibration of FG beam utilizing different types of beam theories: A comparative study", *Comput. Concr.*, **26**(3), 285-292. https://doi.org/10.12989/cac.2020.26.3.285

Alsubaie, A.M., Al-Osta, M.A., Alfaqih, I., Tounsi, A., Chikh, A., Mudhaffar, I.M., Al-Dulaijan, S.U. and Tahir, S. (2024), "Influences of porosity distributions on bending and buckling behaviour of functionally graded carbon nanotube-reinforced composite beam", *Comput. Concr.*, **34**(2), 179-193. https://doi.org/10.12989/cac.2024.34.2.179

Alsubaie, A.M., Alfaqih, I., Al-Osta, M.A., Tounsi, A., Chikh, A., Mudhaffar, I.M. and Tahir, S. (2023), "Porosity-dependent vibration investigation of functionally graded carbon nanotube-reinforced composite beam", *Comput. Concr.*, **32**(1), 75-85. https://doi.org/10.12989/cac.2023.32.1.075

Belabed, Z., Tounsi, A., Bousahla, A.A., Tounsi, A., Khedher, K.M. and Salem, M.A. (2024), "Mechanical behavior analysis of FG-CNTRC porous beams resting on Winkler and Pasternak elastic foundations: A finite element approach", *Comput. Concr.*, **34**(4), 447-476. https://doi.org/10.12989/cac.2024.34.4.447

Berghouti, H., Adda Bedia, E.A., Benkhedda, A. and Tounsi, A. (2019), "Vibration analysis of nonlocal porous nanobeams made of functionally graded material", *Adv. Nano Res.*, **7**(5), 351-364. https://doi.org/10.12989/anr.2019.7.5.351

Bhardwaj, S. and Mishra, D.K. (2024), "Effect of different strut thickness on the mechanical behaviour of 3D printed auxetic structures", *Mater. Today Proc.*, In Press. https://doi.org/10.1016/j.matpr.2024.04.096.

Boggarapu, V., Gujjala, R., Ojha, S., Acharya, S., Venkateswara babu, P., Chowdary, S. and Kumar Gara, D. (2021), "State of the art in functionally graded materials", *Compos. Struct.*, **262**, 113596. https://doi.org/10.1016/j.compstruct.2021.113596

Bose, A., Sathujoda, P. and Canale, G. (2023), "Natural frequency analysis of a functionally graded rotor-bearing system with a slant crack subjected to thermal gradients", *Int. J. Turbo Jet-Engines*, **40**(3), 243-255. https://doi.org/10.1515/tjj-2021-0002

Bouafia, K., Selim, M.M., Bourada, F., Bousahla, A.A., Bourada, M., Tounsi, A., Adda Bedia, E.A. and Tounsi, A. (2021), "Bending and free vibration characteristics of various compositions of FG plates on elastic foundation via quasi 3D HSDT model", *Steel Compos. Struct.*, **41**(4), 487-503. https://doi.org/10.12989/scs.2021.41.4.487

Boutaleb, S., Boulal, A., Zidour, M., Al-Osta, M.A., Tounsi, A. and Tounsi, A. (2024), "On the buckling response of functionally graded carbon nanotube-reinforced composite imperfect beams", *Periodica Polytechnica Civil Engineering*, **68**(4). https://doi.org/10.3311/PPci.23825

Bui, T.Q., Nguyen, N.T., Lich, L.V., Nguyen, M.N. and Truong, T.T. (2018), "Analysis of transient dynamic fracture parameters of cracked functionally graded composites by improved meshfree methods", *Theor. Appl. Fract. Mech.*, **96**, 642-657. https://doi.org/10.1016/j.tafmec.2017.10.005

Burlayenko, V.N., Altenbach, H., Sadowski, T. and Dimitrova, S.D. (2016), "Computational simulations of thermal shock cracking by the virtual crack closure technique in a functionally graded plate", *Comput. Mater. Sci.*, **116**, 11-21. https://doi.org/10.1016/j.commatsci.2015.08.038

Chang, W., Rose, L.R.F., Sha, Z., Huang, F., Kinloch, A.J. and Wang, C.H. (2024), "Multiscale modelling of nanoparticle toughening in epoxy: Effects of particle-matrix interface, particle size, and volume fraction", *Compos. Sci. Technol.*, 110788. https://doi.org/10.1016/j.compscitech.2024.110788

Chen, B., Lin, B., Yang, Y., Zhao, X. and Li, Y. (2022), "Analytical solutions of nonlocal forced vibration of a functionally graded double-nanobeam system interconnected by a viscoelastic layer", *Zeitschrift für Naturforschung A*, **77**(9), 851-873. https://doi.org/10.1515/zna-2022-0059

Chen, Y.F. and Erdogan, F. (1996), "The interface crack problem for a nonhomogeneous coating bonded to a homogeneous substrate", *Mech. Phys. Layer. Grade. Mater.*, **44**(50), 771-787. https://doi.org/10.1016/0022-5096(96)00002-6

Chiong, I., Ooi, E.T., Song, C. and Tin-Loi, F. (2014), "Computation of dynamic stress intensity factors in cracked functionally graded materials using scaled boundary polygons", *Eng. Fract. Mech.*, **131**, 210-231. https://doi.org/10.1016/j.engfracmech.2014.07.030

Cottrell, J.A., Reali, A., Bazilevs, Y. and Hughes, T.J.R. (2006), "Isogeometric analysis of structural vibrations", *Comput. Meth. Appl. Mech. Eng.*, **195**(41-43), 5257-5296. https://doi.org/10.1016/j.cma.2005.09.027

Do, V.N.V. and Lee, C.H. (2019), "Free vibration analysis of FGM plates with complex cutouts by using quasi-3D isogeometric approach", *Int. J. Mech. Sci.*, **159**, 213-233. https://doi.org/10.1016/j.ijmecsci.2019.05.034

Duc, N.D. and Minh, P.P. (2021), "Free vibration analysis of cracked FG CNTRC plates using phase field theory", *Aerosp. Sci. Technol.*, **112**, 106654. https://doi.org/10.1016/j.ast.2021.106654

Ebrahimi, F. and Jafari, A. (2017), "Investigating vibration behavior of smart imperfect functionally graded beam subjected to magnetic-electric fields based on refined shear deformation theory", *Adv. Nano Res.*, **5**(4), 281-301. https://doi.org/10.12989/anr.2017.5.4.281

Friswell, M.I. and Penny, J.E.T. (2002), "Crack modeling for structural health monitoring", *Struct. Health Monit.*, **1**(2), 139-148. https://doi.org/10.1177/1475921702001002002

Garima, Mishra, D.K., Singh, R.K. and Gupta, D. (2024), "Experimental investigation into the fabrication of porous scaffolds for biomedical applications using electrospinning", *Materials Today: Proceedings*, In Press. https://doi.org/10.1016/j.matpr.2024.05.035

Gawah, Q., Bourada, F., Al-Osta, M.A., Tahir, S.I., Tounsi, A. and Yaylaci, M. (2024), "An improved first-order shear deformation theory for wave propagation analysis in FG-CNTRC beams resting on a viscoelastic substrate", *Int. J. Struct. Stabil. Dyn.*, https://doi.org/10.1142/S0219455425500105

Gupta, A., Jain, N.K., Salhotra, R. and Joshi, P.V. (2018), "Effect of crack location on vibration analysis of partially cracked isotropic and FGM micro-plate with non-uniform thickness: An analytical approach", *Int. J. Mech. Sci.*, **145**, 410-429. https://doi.org/10.1016/j.ijmecsci.2018.07.015

Hadji, L. and Avcar, M. (2021), "Nonlocal free vibration analysis of porous FG nanobeams using hyperbolic shear deformation beam theory", *Adv. Nano Res.*, **10**(3), 281-293. https://doi.org/10.12989/anr.2021.10.3.281

Hadji, L., Avcar, M. and Civalek, Ö. (2021), "An analytical solution for the free vibration of FG nanoplates", *J. Brazil. Soc. Mech. Sci. Eng.*, **43**(9), 418. https://doi.org/10.1007/s40430-021-03134-x

Hadji, L., Avcar, M. and Civalek, Ö. (2022), "Free vibration of carbon nanotube-reinforced composite beams under the various boundary conditions", *Adv. Compos. Mater. Struct.*, 87-108.

Hadji, L., Plevris, V., Madan, R. and Ait Atmane, H. (2024), "Multi-directional functionally graded sandwich plates: Buckling and free vibration analysis with refined plate models under various boundary conditions", *Computation*, **12**(4), 65. https://doi.org/10.3390/computation12040065

Huang, S.J., Kannaiyan, S. and Subramani, M. (2022), "Effect of nano-Nb_2O_5 on the microstructure and mechanical properties of AZ31 alloy matrix nanocomposites", *Adv. Nano Res.*, **13**(4), 407-416. https://doi.org/10.12989/anr.2022.13.4.407

Hughes, T.J.R., Cottrell, J.A. and Bazilevs, Y. (2005), "Isogeometric analysis: CAD, finite elements, NURBS, exact geometry and mesh refinement", *Comput. Meth. Appl. Mech. Eng.*, **194**(39-41), 4135-4195. https://doi.org/10.1016/j.cma.2004.10.008

Jweeg, M.J., Njim, E. K., Abdullah, O.S., Al-Shammari, M.A., Al-Waily, M. and Bakhy, S.H. (2023), "Free vibration analysis of composite cylindrical shell reinforced with silicon nanoparticles: Analytical and FEM approach", *Phys. Chem. Solid State*, **24**(1), 26-33. https://doi.org/10.15330/pcss.24.1.26-33

Kanu, N.J., Vates, U.K., Singh, G.K. and Chavan, S. (2019), "Fracture problems, vibration, buckling, and bending analyses of functionally graded materials: A state-of-the-art review including smart FGMS", *Particul. Sci. Technol.*, **37**(5), 583-608. ttps://doi.org/10.1080/02726351.2017.1410265

Ke, L., Wang, Y., Yang, J., Kitipornchai, S. and Alam, F. (2012), "Nonlinear vibration of edged cracked FGM beams using differential quadrature method", *Sci. China Phys. Mech. Astr.*, **55**(11), 2114-2121. https://doi.org/10.1007/s11433-012-4704-y

Ke, L.L., Yang, J., Kitipornchai, S. and Xiang, Y. (2009), "Flexural vibration and elastic buckling of a cracked Timoshenko beam made of functionally graded materials", *Mech. Adv. Mater. Struct.*, **16**(6), 488-502. https://doi.org/10.1080/15376490902781175

Khiem, N.T., Hai, T.T. and Huong, L.Q. (2023), "Modal analysis of cracked FGM beam with piezoelectric layer", *Mech. Based Des. Struct.*, **51**(9), 5120-5140. https://doi.org/10.1080/15397734.2021.1992775

Khiem, N.T., Tran, H.T. and Nam, D. (2020), "Modal analysis of cracked continuous Timoshenko beam made of functionally graded material", *Mech. Based Des. Struct.*, **48**(4), 459-479. https://doi.org/10.1080/15397734.2019.1639518

Kolman, R., Sorokin, S., Bastl, B., Kopačka, J. and Plešek, J. (2015), "Isogeometric analysis of free vibration of simple shaped elastic samples", *J. Acoust. Soc. Am.*, **1379**(4), 2089-2100. https://doi.org/10.1121/1.4916199

Kou, K.P. and Yang, Y. (2019), "A meshfree boundary-domain integral equation method for free vibration analysis of the

functionally graded beams with open edged cracks", *Compos. Part B Eng.*, **156**, 303-309. https://doi.org/10.1016/j.compositesb.2018.08.089

Kouider, D., Kaci, A., Selim, M.M., Bousahla, A.A., Bourada, F., Tounsi, A., Tounsi, A. and Hussain, M. (2021), "An original four-variable quasi-3D shear deformation theory for the static and free vibration analysis of new type of sandwich plates with both FG face sheets and FGM hard core", *Steel Compos. Struct.*, **41**(2), 167-191. http://doi.org/10.12989/scs.2021.41.2.167

Kuma, Y., Gupta, A. and Tounsi, A. (2021), "Size-dependent vibration response of porous graded nanostructure with FEM and nonlocal continuum model", *Adv. Nano Res.*, **11**(1), 1-17. https://doi.org/10.12989/anr.2021.11.1.001

Kumar, H., Bhardwaj, K., Nepovimova, E., Kuča, K., Singh Dhanjal, D., Bhardwaj, S., Bhatia, S.K., Verma, R. and Kumar, D. (2020), "Antioxidant functionalized nanoparticles: A combat against oxidative stress", *Nanomaterials*, **10**(7).

Lafi, D.E., Bouhadra, A., Mamen, B., Menasria, A., Bourada, M., Bousahla, A.A., Bourada, F., Tounsi, A., Tounsi, A. and Yaylaci, M. (2024), "Combined influence of variable distribution models and boundary conditions on the thermodynamic behavior of FG sandwich plates lying on various elastic foundations", *Struct. Eng. Mech.*, **89**(2), 103-119. https://doi.org/10.12989/sem.2024.89.2.103

Li, X., Wang, T., Liu, F. and Zhu, Z. (2021), "Computer simulation of the nonlinear static behavior of axially functionally graded microtube with porosity", *Adv. Nano Res.*, **11**(4), 437-451. https://doi.org/10.12989/anr.2021.11.4.437

Lien, T.V., Duc, N.T. and Khiem, N.T. (2017), "Free vibration analysis of multiple cracked functionally graded Timoshenko beams", *Latin Am. J. Solids Struct.*, **14**(9), 1752-1766.

Lin, B., Chen, B., Li, Y. and Yang, J. (2021), "Vibration characteristics and stable region of a parabolic FGM thin-walled beam with axial and spinning motion", *Zeitschrift für Naturforschung A*, **76**(9), 787-798. https://doi.org/10.1515/zna-2021-0073

Liu, S., Yu, T., Van Lich, L., Yin, S. and Bui, T.Q. (2018), "Size effect on cracked functional composite micro-plates by an XIGA-based effective approach", *Meccanica*, **53**(10), 2637-2658. https://doi.org/10.1007/s11012-018-0848-9

Madan, R., Khobragade, P. and Bhowmick, S. (2024), "Impact of porosity on free vibration and limit analysis of power-law-based functionally graded disks", *Multidiscipl. Model. Mater. Struct.*, **20**(6), 1192-1212.

Madenci, E., Özkiliç, Y.O., Hakamy, A. and Tounsi, A. (2023), "Experimental tensile test and micro-mechanic investigation on carbon nanotube reinforced carbon fiber composite beams", *Adv. Nano Res.*, **14**(5), 443-450. https://doi.org/10.12989/anr.2023.14.5.443

Mangalasseri, A.S., Mahesh, V., Mukunda, S., Mahesh, V., Ponnusami, S.A., Harursampath, D. and Tounsi, A. (2023), "Vibration based energy harvesting performance of magneto-electro-elastic beams reinforced with carbon nanotubes", *Adv. Nano Res.*, **14**(1), 27-43. https://doi.org/10.12989/anr.2023.14.1.027

Monfared, M.M. and Ayatollahi, M. (2013), "Dynamic stress intensity factors of multiple cracks in an orthotropic strip with FGM coating", *Eng. Fract. Mech.*, **109**, 45-57. https://doi.org/10.1016/j.engfracmech.2013.07.002

Mudhaffar, I.M., Chikh, A., Tounsi, A., Al-Osta, M.A., Al-Zahrani, M.M. and Al-Dulaijan, S.U. (2023), "Impact of viscoelastic foundation on bending behavior of FG plate subjected to hygro-thermo-mechanical loads", *Struct. Eng. Mech.*, **86**(2), 167-180. https://doi.org/10.12989/sem.2023.86.2.167

Nasirmanesh, A. and Mohammadi, S. (2017), "An extended finite element framework for vibration analysis of cracked FGM shells", *Compos. Struct.*, **180**, 298-315. https://doi.org/10.1016/j.compstruct.2017.08.019

Natarajan, S., Baiz, P.M., Bordas, S., Rabczuk, T. and Kerfriden, P. (2011), "Natural frequencies of cracked functionally graded material plates by the extended finite element method", *Compos. Struct.*, **93**(11), 3082-3092. https://doi.org/10.1016/j.compstruct.2011.04.007

Neamah, R.A., Nassar, A.A. and Alansari, L.S. (2022), "Modeling and analyzing the free vibration of simply supported functionally graded beam", *J. Aerosp. Technol. Manag.*, **14**, e1522.

Neamah, R.A., Al-Raheem, S.K., Njim, E. K., Abboud, Z. and Al-Ansari, L S. (2024), "Experimental and numerical investigation of the natural frequency for the intact and cracked laminated composite beam", *J. Aerosp. Technol. Manage.*, **16**. https://doi.org/10.1590/jatm.v16.1337

Njim, E.K., Hasan, H.R., Jweeg, M.J., Al-Waily, M., Hameed, A. A., Youssef, A.M. and Elsayed, F.M. (2024), "Mechanical properties of sandwiched construction with composite and hybrid core structure", *Adv. Polym. Technol.*, **2024**, 1-14. https://doi.org/10.1155/2024/3803199

Raad, H., Najim, E., Jweeg, M., AlWaily, M., Hadji, L. and Madan, R. (2024), "Vibration analysis of sandwich plates with hybrid composite cores combining porous polymer and foam structures", *J. Comput. Appl. Mech.*, **55**(3). https://doi.org/10.22059/jcamech.2024.377658.1121

Raju Rallabandi, S., Pilla, D.P., Dowluru, S., Palli, S., Sharma, N., Sharma, S.K. and Sharma, R.C. (2024), "Critical evaluation of epoxy-hemp-pineapple-palm fiber composites using hybrid AHM-TOPSIS technique for sustainable structural applications", *J. Chinese Inst. Eng.*, **47**(3), 1-12. https://doi.org/10.1080/02533839.2024.2308250.

Shabani, S. and Cunedioglu, Y. (2020), "Free vibration analysis of functionally graded beams with cracks", *J. Appl. Comput. Mech.*, **6**(4), 908-919. https://doi.org/10.1080/02533839.2024.2308250

Sharma, R.C., Gopala Rao, L.V.V., Srikar, B., Palli, S., Naidu, Y.A., Sharma, N. and Sharma. S.K. (2024), "Investigation of the dynamic behavior of hybrid composites using Finite Element and experimental method", *J. Chinese Inst. Eng.*, **47**, In Press.

Sharma, S.K., Sharma, R.C., Choi, Y. and Lee, J. (2023), "Experimental and mathematical study of flexible-rigid rail vehicle riding comfort and safety", *Appl. Sci.*, **13**(9), 5252. https://doi.org/10.3390/app13095252

Sherafatnia, K., Farrahi, G.H. and Faghidian, S.A. (2014), "Analytic approach to free vibration and buckling analysis of functionally graded beams with edge cracks using four engineering beam theories", *Int. J. Eng.*, **27**(6), 979-990.

Şimşek, M. and Yurtcu, H.H. (2013), "Analytical solutions for bending and buckling of functionally graded nanobeams based on the nonlocal Timoshenko beam theory", *Compos. Struct.*, **97**, 378-386. https://doi.org/10.1016/j.compstruct.2012.10.038

Singh, H., Singh, J.I.P., Singh, S., Dhawan, V. and Tiwari, S.K. (2018), "A brief review of jute fibre and its composites", *Mater. Today Proc.*, **5**(14), 28427-28437. https://doi.org/10.1016/j.matpr.2018.10.129

Singh, S.K., Sondhi, L., Sahu, R.K., Madan, R. and Yadav, S. (2024), "Investigating thermo-mechanical stresses in functionally graded disks using Navier's method for different loading conditions", *Struct. Eng. Mech.*, **91**(6), 627-642. https://doi.org/10.12989/sem.2024.91.6.627

Sinha, G.P. and Kumar, B. (2021), "Review on vibration analysis of functionally graded material structural components with cracks", *J. Vib. Eng. Technol.*, **9**(1), 23-49. https://doi.org/10.1007/s42417-020-00208-3

Soni, V.K., Sahu, R.K., Sinha, A.K. and Madan, R. (2024),

Development and Characterization of Microwave Sintered SiC Reinforced 3003 Aluminium Alloy, In *Composite Materials Processing Using Microwave Heating Technology*, 185-199, Springer Nature Singapore, Singapore.

Tahir, S.I., Tounsi, A., Chikh, A., Al-Osta, M.A., Al-Dulaijan, S.U. and Al-Zahrani, M.M. (2022), "The effect of three-variable viscoelastic foundation on the wave propagation in functionally graded sandwich plates via a simple quasi-3D HSDT", *Steel Compos. Struct.*, **42**(4), 501-511. https://doi.org/10.12989/scs.2022.42.4.501

Tam, M., Yang, Z., Zhao, S. and Yang, J. (2019), "Vibration and buckling characteristics of functionally graded graphene nanoplatelets reinforced composite beams with open edge cracks", *Materials*, **12**(9). https://doi.org/10.3390/ma12091412

Tounsi, A., Bousahla, A.A., Tahir, S.I., Mostefa, A.H., Bourada, F., Al-Osta, M.A. and Tounsi, A. (2024), "Influences of different boundary conditions and hygro-thermal environment on the free vibration responses of FGM sandwich plates resting on viscoelastic foundation", *Int. J. Struct. Stabil. Dyn.*, **24**(11), 2450117. https://doi.org/10.1142/S0219455424501177

Tounsi, A., Hadj Mostefa, A., Attia, A., Bousahla, A.A., Bourada, F., Tounsi, A. and Al-Osta, M.A. (2023a), "Free vibration investigation of functionally graded plates with temperature-dependent properties resting on a viscoelastic foundation", *Struct. Eng. Mech.*, **86**(1), 1-16. https://doi.org/10.12989/sem.2023.86.1.001

Tounsi, A., Hadj Mostefa, A., Bousahla, A.A., Tounsi, A., Ghazwani, M.H., Bourada, F. and Bouhadra, A. (2023b), "Thermodynamical bending analysis of P-FG sandwich plates resting on nonlinear visco-Pasternak's elastic foundations", *Steel Compos. Struct.*, **49**(3), 307-323. https://doi.org/10.12989/scs.2023.49.3.307

Tounsi, A., Tahir, S.I., Al-Osta, M.A., Do-Van, T., Bourada, F., Bousahla, A.A. and Tounsi, A. (2023c), "An integral quasi-3D computational model for the hygro-thermal wave propagation of imperfect FGM sandwich plates", *Comput. Concr.*, **32**(1), 61-74. https://doi.org/10.12989/cac.2023.32.1.061

Viola, E., Tornabene, F. and Fantuzzi, N. (2013), "Generalized differential quadrature finite element method for cracked composite structures of arbitrary shape", *Compos. Struct.*, **106**, 815-834. https://doi.org/10.1016/j.compstruct.2013.07.034

Yang, E.C., Zhao, X. and Li, Y.H. (2015), "Free vibration analysis for cracked fgm beams by means of a continuous beam model", *Shock Vib.*, **1**, 197049. https://doi.org/10.1155/2015/197049

Yang, J. and Chen, Y. (2008), "Free vibration and buckling analyses of functionally graded beams with edge cracks", *Compos. Struct.*, **83**(1), 48-60. https://doi.org/10.1016/j.compstruct.2007.03.006

Yu, Z. and Chu, F. (2009), "Identification of crack in functionally graded material beams using the p-version of finite element method", *J. Sound Vib.*, **325**(1), 69-84. https://doi.org/10.1016/j.jsv.2009.03.010

Zhang, Ch., Savaidis, A., Savaidis, G. and Zhu, H. (2003), "Transient dynamic analysis of a cracked functionally graded material by a BIEM", *Proceedings of the 11th International Workshop on Computational Mechanics of Materials*, **26**, 167-174.

Zhang, Y.W., Ding, H.X., She, G.L. and Tounsi, A. (2023), "Wave propagation of CNTRC beams resting on elastic foundation based on various higher-order beam theories", *Geomech. Eng.*, **33**(4), 381-391. https://doi.org/10.12989/gae.2023.33.4.381